Received: 6 September 2020 | Accepted: 23 November 2020 | Published online: 12 January 2021

DOI: 10.1002/vzj2.20096

Vadose Zone Journal

ORIGINAL RESEARCH ARTICLE

On the laboratory calibration of dielectric permittivity models for agricultural soils: Effect of systematic porosity variation

Xicai Pan[1] | **Yudi Han**[1,2] | **Kwok Pan Chun**[3] | **Jiabao Zhang**[1] | **Donghao Ma**[1] | **Hongkai Gao**[4]

[1] State Key Lab. of Soil and Sustainable Agriculture, Institute of Soil Science, Chinese Academy of Sciences, Nanjing 210008, China

[2] Univ. of the Chinese Academy of Sciences, Beijing 100049, China

[3] Dep. of Geography, Hong Kong Baptist Univ., Hong Kong, China

[4] School of Geographical Sciences, East China Normal Univ., Shanghai 200241, China

Correspondence
Xicai Pan and Jiabao Zhang, State Key Lab. of Soil and Sustainable Agriculture, Institute of Soil Science, Chinese Academy of Sciences, Nanjing, 210008, China.
Email: xicai.pan@issas.ac.cn; jbzhang@issas.ac.cn

Assigned to Associate Editor Hailong He.

Funding information
National Natural Science Foundation of China, Grant/Award Numbers: 41771262, 41671228

Abstract

Dielectric techniques are fundamental methods for measuring soil water content, and they commonly rely on the conventional laboratory calibration of the dielectric permittivity models between a dielectric constant and water content. As a non-negligible factor, porosity has been constructed differently in some models as a calibration constant, but the systematic porosity variations during the laboratory model calibration and field applications are not yet well addressed. Based on time-domain reflectometer laboratory calibration experiments, this study investigated this issue using three preestablished dielectric permittivity models: the Purdue calibration equation (American Society for Testing and Materials model [ASTM]), the complex refractive index model (CRIM), and a piecewise CRIM model (CRIMP). Results demonstrate that a generalized porosity constant used in the calibration would bring in additional structural bias compared with the calibration using variable porosities, and its magnitude varies with the model structure. The deviation of the generalized porosity constant can further amplify the structural bias of ASTM and CRIM for soils with low clay content, but it is insensitive for the soils with high clay content due to the overwhelming role of model structure error. Only the model CRIMP with a "perfect" model structure can effectively cope with the systematic porosity variation and keep a stable built-in capability for estimating calibration constants from readily available soil data. These findings highlight ignoring porosity variation should not be taken for granted for calibrating and applying the preestablished models.

1 | INTRODUCTION

The dielectric measurement techniques operating at high frequency such as time domain reflectometry (TDR), ground-penetrating radar (GPR), and microwave remote sensing (Huisman, Hubbard, Redman, & Annan, 2003; McNairn, Pultz, & Boisvert, 2002; Robinson et al., 2008) are fundamental approaches for measuring soil water content at various scales. These soil water measurement methods are based on the substantial difference between dielectric constants of water, minerals, and air. There are a variety of petrophysical models developed to relate the measured bulk dielectric constant to soil water content. Considering the complex interactions between soil and water (Chen & Or, 2006), modeling the dielectric conditions of wet soils requires experimentally

Abbreviations: ASTM, American Society for Testing and Materials model; CRIM, complex refractive index model; CRIMP, piecewise complex refractive index model; GPR, ground-penetrating radar; MAE, mean absolute error; MSD, mean standard deviation; SEE, standard error of estimate; TDR, time-domain reflectometry; TOPP, Topp model.

determined model constants—namely, calibration—for different soils. However, the direct field calibration of the petrophysical model for site-specific soil is the most accurate approach for measuring soil water content, but it is seldom used due to labor-intensive auxiliary measurements. Alternatively, a variety of preestablished dielectric permittivity models derived from laboratory experiments are widely used due to its accessibility and versatility (Robinson, Jones, Wraith, Or, & Friedman, 2003; Roth, Malicki, & Plagge, 1992).

Soil porosity has been identified as an important role in modeling soil dielectric behavior and has been constructed in most preestablished dielectric permittivity models. The empirical determination of material-specific calibration equations usually directly includes soil porosity or dry bulk density (Jacobsen & Schjonning, 1993; Drnevich, Ashmawy, Yu, & Sallam, 2005; Malicki, Plgge, & Roth, 1996). With more understanding of multiphysical processes arising from the soil–water dielectric interactions, theoretical mixing models were developed to link dielectric constants of each phase with their volumetric fractions. Commonly, the simple three-phase mixing models work well for quantifying the bulk dielectric constant of low dielectric-loss soils (Birchak, Gardner, Hipp, & Victor, 1974; Roth, Schulin, Fluhler, & Attinger, 1990; Weitz, Grauel, Keller, & Veldkamp, 1997). Since the dielectric constant of bound water is much lower than that of free water (Dobson, Ulaby, Hallikainen, & El-Rayes, 1985), its role becomes non-negligible for quantifying dielectric mediate loss soils with notable bounding water. Thus, more advanced four-phase models were proposed to cover a wider range of applicability (Dobson et al., 1985; Friedman, 1998; Ponizovsky, Chudinovaa, & Pachepsky, 1999). In fact, no matter whether the porosity is defined as a constant or a variable in the dielectric permittivity models, it is often impractical to obtain the porosity values at the field conditions with temporal variation. Normally, just representative values are used to derive the empirical or semiempirical relationships from specific laboratory calibrations.

For the laboratory calibration of dielectric permittivity models for specific soil, there are two commonly used approaches for controlling soil water conditions. One is to produce soil samples with different specific water content values ranging from air dry to near water saturation. The wetted soil samples need to be compacted in the sample container, but the bulk density (the soil porosity) usually changes with water content, according to soil compaction theory (Das, 2008). The other approach is to produce soil samples with continuously varying water contents via drainage and evaporation. The soil porosity may also change with water content due to swelling–shrinkage process, especially for the fine-textured soils such as loess and expansive soils (Fleureau, Kheirbek-Saoud, Soemitro, & Taibi, 1993). Furthermore, in situ soil porosity change of plow-layer soils is more noteworthy than in the laboratory due to natural and anthropogenic factors such as wetting–drying, freezing–thawing, and plowing (Alakukku et al., 2003; Alaoui, Lipiec, & Gerke, 2011; Fabiola, Giarola, da Silva, Imhoff, & Dexter, 2003; Radford et al., 2000). These patterned porosity changes are hereinafter referred to as systematic porosity variation. However, a constant porosity is usually employed both in laboratory calibration and field application. The influences of the porosity variation on the estimation are still not well investigated, in both laboratory and field conditions. In addition, how to choose a representative value for the porosity and its impact on the measurement accuracy of different dielectric permittivity models are well assessed for different soils. Hence, research on the effect of soil water-related processes like compaction and shrinkage on the dielectric behavior of different soils in laboratory calibration would be very helpful to bridge the gap between laboratory calibration and field application (Schwing, Scheuermann, & Wagner, 2010; Steelman & Endres, 2011; Thomas, Chapman, Rogers, & Metje, 2010a, 2010b).

Core Ideas

- Systematic porosity variation is noteworthy for dielectric measurement techniques.
- Impacts of porosity generalization on model calibration vary with model structure and soil type.
- Caution is needed for calibrating and applying preestablished models for agricultural soils.

In this study, we take four dielectric permittivity models with different degrees of porosity representation for illustration purposes. The effect of porosity change with the degree of water saturation on the conventional calibration of TDR measurements is investigated using eight different soils. The specific objectives are (a) to diagnose the role of systematic porosity variation in the structural residuals between water content observations and model estimates; and (b) to find practical solutions to cope with the water content measurements in the agricultural soils with systematic porosity variation.

2 | MATERIALS AND METHODS

2.1 | Laboratory measurements

The eight soils in Table 1 were sampled from the upper 30 cm of the A horizon in the agricultural lands with different genesis environments in China. The soil texture information was obtained from a laser diffraction particle size analyzer (Beckman Coulter LS 13320). The soil organic

TABLE 1 Physical properties of eight soil samples in China

Part	Soil no.	Texture[a]/classification[b]	Location	Clay	Silt	Sand	SOM[c]
				%			
Part 1	S1	Sandy loam/Aridi-Sandic Primosols	Henan	14.4	4.8	80.8	0.36
	S2	Sandy loam/Siltigi-Ustic Cambosols	Xinjiang	14.7	15.0	70.2	0.80
	S3	Silt loam/Loessi-Orthic Primosols	Shanxi	22.6	53.6	23.8	0.25
	S4	Loam/Ochri-Aquic Cambosols	Henan	26.2	31.2	42.6	0.94
Part 2	S5	Silty clay loam /Hapli-Ustic Cambosols	Gansu	35.7	47.2	17.1	1.53
	S6	Clay/Hapli-Udic Isohumosols	Heilongjiang	40.8	35.9	23.3	2.69
	S7	Clay/Ali-Udic Argosols	Jiangxi	51.1	27.0	21.9	1.09
	S8	Silty clay/Shajiang Calci-Aquic Vertosols	Anhui	51.3	41.1	7.6	1.82

[a]The USDA classification.
[b]The Chinese soil taxonomy (ISS, 2001).
[c]SOM, soil organic matter.

TABLE 2 Four dielectric permittivity models

Model	Equation	Calibration constants	Known constants
TOPP, Topp et al. (1980)		$\theta = -5.3 \times 10^{-2} + 2.92 \times 10^{-2}\varepsilon_b - 5.5 \times 10^{-4}\varepsilon_b^2 + 4.3 \times 10^{-6}\varepsilon_b^3$	none
ASTM, Drnevich et al. (2005)	$\sqrt{\varepsilon_b} = a\frac{\rho_s(1-\Phi)}{\rho_w} + b\theta$	a, b	Φ, $\rho_s = 2.65$ g cm^{-3}, $v = 1.0$ g cm^{-3}
CRIM, Birchak et al. (1974)	$\varepsilon_b^\alpha = (1-\Phi)\varepsilon_s^\alpha + \theta\varepsilon_w^\alpha + (\Phi-\theta)\varepsilon_a^\alpha$	ε_s, α	Φ, $\varepsilon_a = 1$, $\varepsilon_w = 78$
CRIMP, Ponizovsky et al. (1999)	$\varepsilon_b^\alpha = \begin{cases}(1-\Phi)\varepsilon_s^\alpha + \theta\varepsilon_c^\alpha + (\Phi-\theta)\varepsilon_a^\alpha, \theta < \theta_{c,max}\\ (1-\Phi)\varepsilon_s^\alpha + \theta_{c,max}\varepsilon_c^\alpha + (\theta-\theta_{c,max})\varepsilon_w^\alpha + (\Phi-\theta)\varepsilon_a^\alpha,\ \theta \geq \theta_{c,max}\end{cases}$	ε_c, $\theta_{c,max}$, α	Φ, $\varepsilon_s = 4$, $\varepsilon_a = 1$, $\varepsilon_w = 78$

Note. TOPP, the Topp model; ASTM, American Society for Testing and Materials model; CRIM, the complex refractive index model; CRIMP, a piecewise CRIM model. θ and $\theta_{c,max}$ and the total volumetric water content and the maximum volumetric content of bound water, respectively; ε_b is the bulk dielectric constant; ε_s, ε_w, ε_c, and ε_a are the dielectric constants of solid phase, free water, bound water, and air, respectively; ρ_s and ρ_w are the density of soil particle and water; Φ is the soil porosity; α is a geometrical parameter; a and b are free model fitting parameters.

contents were measured using the hydrated heat potassium dichromate oxidation-colorimetry method (Bremner & Jenkinson, 1960). Given the importance of clay content in dielectric permittivity model performance, the eight soils were organized as two groups (Part 1: clay % < 30%, Part 2: clay% > 30%).

2.2 | Dielectric permittivity models

Four representative dielectric permittivity models with different degrees of porosity representation in Table 2 are used in this study. The first model, Topp, Davis, and Annan (1980) (TOPP), was established using specific laboratory calibration with gravimetric sampling. It describes the dielectric permittivity model for a wide range of mineral soils but without considering the effect of soil porosity. The second one, Drnevich et al. (2005) (ASTM), was semiempirically derived from soil specific calibration, and porosity is incorporated via the relation between soil bulk density and the common soil particle density. The last two models, Birchak et al. (1974) (CRIM) and Ponizovsky et al. (1999) (CRIMP), were constructed based on theoretical mixing rules, but the latter does not only consider soil porosity but also bound water effect. Hence, its application range can extend to soils with high clay content.

2.3 | General calibration procedure

To quantify the relationship between soil dielectric constant and volumetric water content for each soil, we made designed samples with a variety of water content from air dried to nearly saturated. For each designed water content, the oven-dried soil samples were placed to a thin layer on a tray and sprayed with certain purified water. Then, soil samples were packed in a beaker with a 10-cm diameter and 20-cm height. Through rough layer by layer compaction, the beaker was

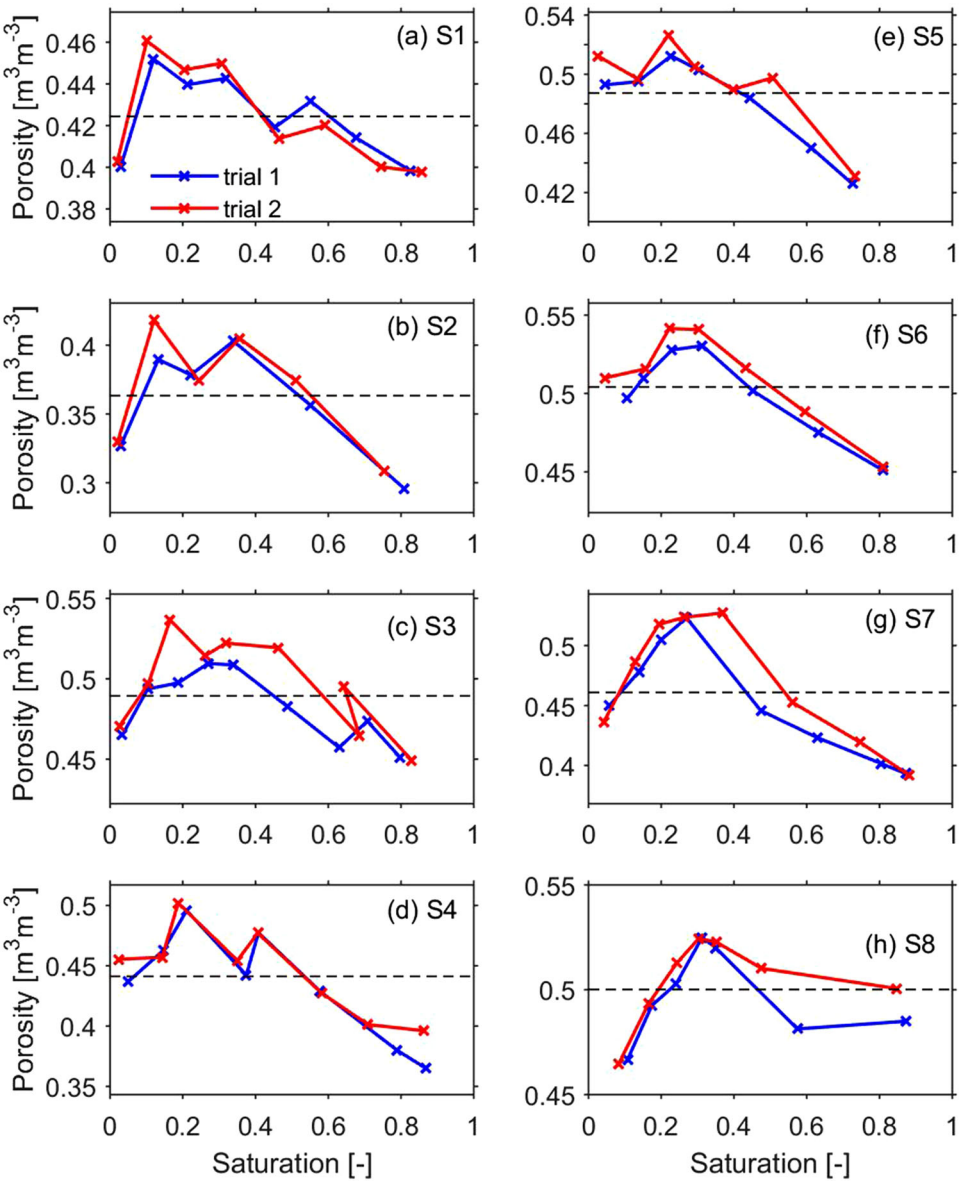

FIGURE 1 Effect of water content on porosity in the repeated calibrations (Trials 1 and 2). The dashed line is the mean value $\bar{\Phi}_r$ (the averaged value of all the estimated porosities) of all samples for each soil

filled up to a height of around 18 cm, and the soil sample surface was then trimmed evenly for determining the sample volume. For replication, another specimen with the same soil samples was made in parallel by another operator. Before each TDR measurement, the specimens were stored at a room temperature of around 24 ˚C over 48 h for equilibrating. After the TDR measurement, the specimens were weighed and then removed from the beakers for oven drying. After oven drying, volumetric water content and porosity were calculated by using a mean particle density of 2.65 g cm^{-3} for common soils (Blanco-Canqui, Lal, Post, Izaurralde, & Shipitalo, 2006).

A recently commercialized sensor TDR315 (Acclima, Meridian) with stainless steel three-element waveguide (15 cm × 3.5 mm) was used to measure soil dielectric constants. It operates the same principles of conventional TDR working in the gigahertz frequency range (Datta et al., 2018). In the experiment, five TDR315 probes were used, and the wave-form data were collected by a CR1000 data-logger (Campbell Scientific). Travel time derived from the wave-form data are based on the tangent-line methods (Evett, 2000; Or, Jones, Van Shaar, Humphries, & Koberstein, 2004). In addition, following Heimovaara (1993) and Robinson et al. (2003), a travel time correction factor t_0 is applied to the travel time evaluation in order to account for the signal travel time within the sensor head. This results in two unknowns: the correction factor t_0, and an electrical length of the probe, L_e. They can be obtained from calibration measurements in air

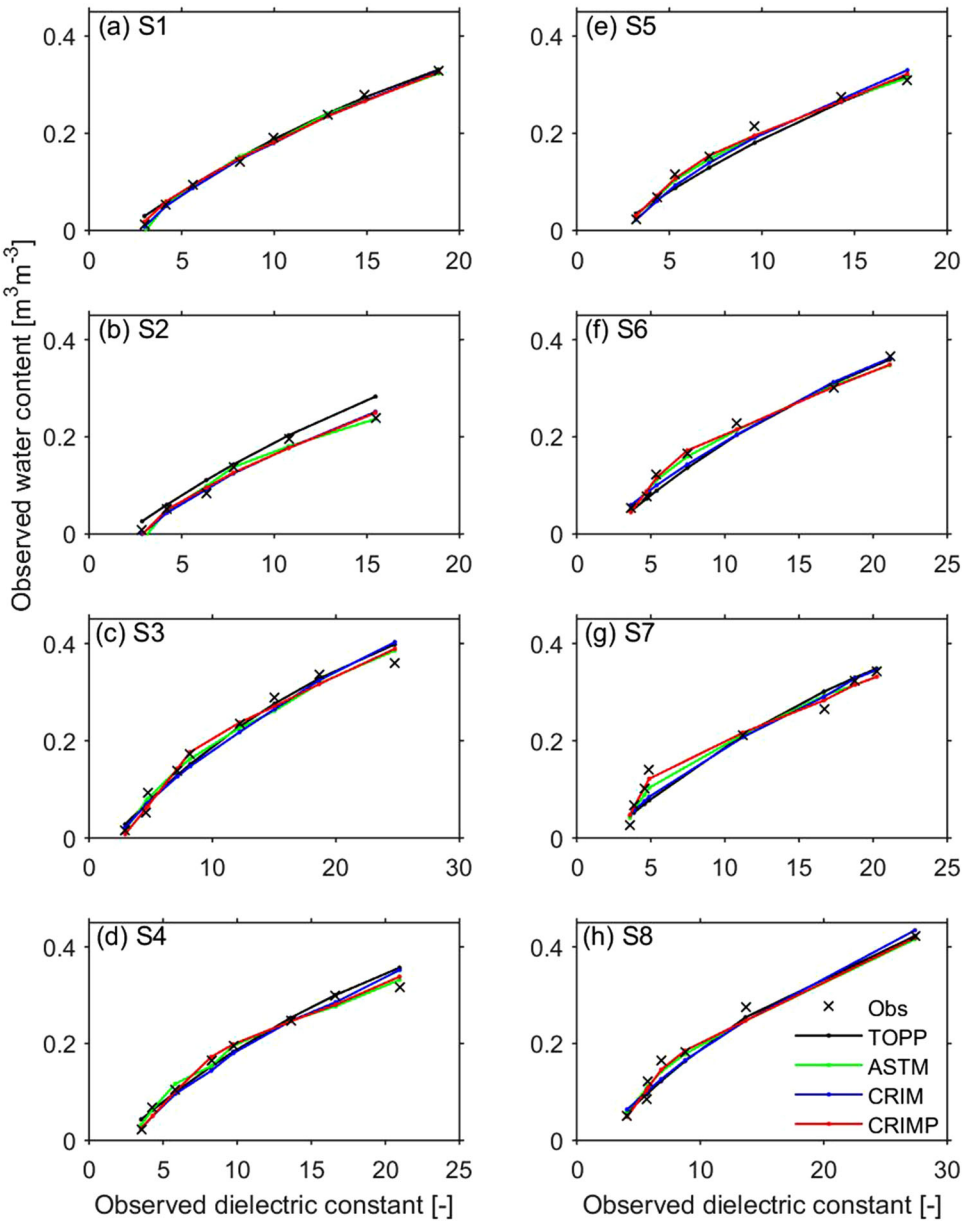

FIGURE 2 Curve fitting of the dielectric constant relationship using four calibration models (the Topp model [TOPP], the American Society for Testing and Materials model [ASTM], the complex refractive index model [CRIM], and a piecewise CRIM model [CRIMP]). Panels a–h are the sampling soils from S1 to S8

and deionized water by solving the two equations

$$t_a = t_0 + 2L_e\sqrt{\varepsilon_a}/c_0 \quad (1)$$

$$t_w = t_0 + 2L_e\sqrt{\varepsilon_w}/c_0 \quad (2)$$

where t_a and t_w are the measured total travel times in air and water, respectively; the known dielectric constant of air and water are set as $\varepsilon_a = 1$ and $\varepsilon_w = 78$ (Kaatze, 1989), respectively; and c_0 is the velocity of electromagnetic signals in free space (0.3 m ns^{-1}).

The procedure for deriving soil dielectric constant is briefly summarized as follows. Firstly, three repeated measurements were recorded for each soil filled beaker, and corresponding travel times t_s are obtained using the above approach. Then, following Equation 1, the soil dielectric constant ε_s was calculated with the mean t_s and other known parameters.

Then, the calibration constants for each model in Table 2 are estimated by fitting the dielectric permittivity model to the observed points, using the sum of squared error (SSE) objective function

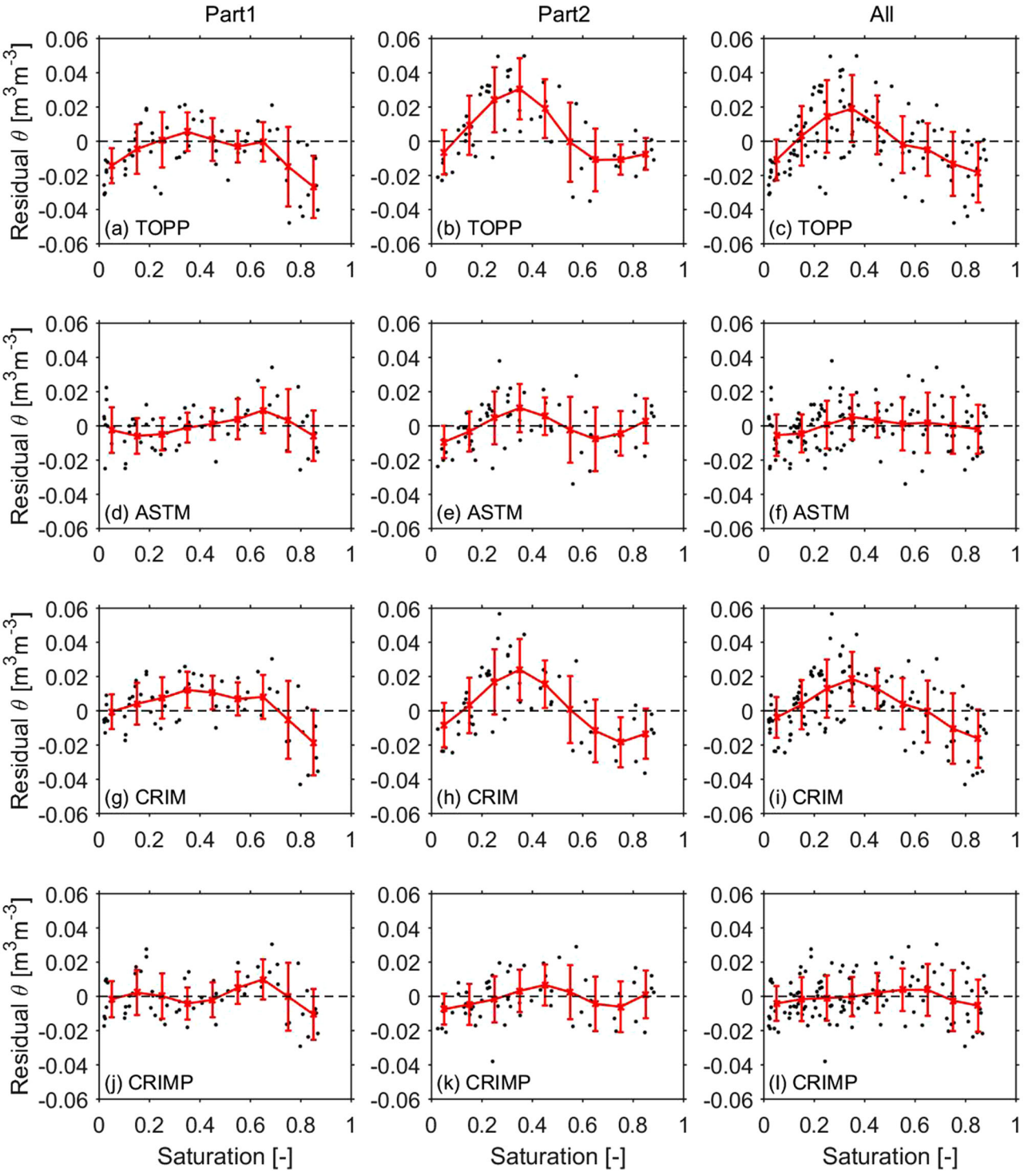

FIGURE 3 Performances of four calibration models (the Topp model [TOPP], the American Society for Testing and Materials model [ASTM], the complex refractive index model [CRIM], and a piecewise CRIM model [CRIMP]) for three groups of soils (Part 1, Part 2, and all). The error structure in red color is presented by the mean and error bar calculated using the residuals $\theta_r - \hat{\theta}_r$ within each bin, where θ_r is the observed volumetric content, and $\hat{\theta}_r$ is the predicted value with the models

$$\mathrm{SSE} = \frac{1}{R}\sum\left(\theta_r - \hat{\theta}_r\right)^2 \tag{3}$$

where θ_r is the observed volumetric content, $\hat{\theta}_r$ is the predicted value with the models, and R is the number of calibration points at different water contents. The calibration constants were optimized using sequential quadratic programming (SQP) algorithm in Octave (GNU Octave 4.4.0), which uses a successive quadratic programming solver. Other known constants directly used in the optimization are also

TABLE 3 Error statistics of model estimates for three groups of soils (Part 1, Part 2, and all) when using variable porosity in calibration

Statistic[a]	Model[b]	Part 1	Part 2	All
		$m^3\ m^{-3}$		
SEE	TOPP	0.018	0.024	0.021
	ASTM	0.013	0.015	0.014
	CRIM	0.016	0.022	0.019
	CRIMP	0.013	0.013	0.013
MAE	TOPP	0.008	0.013	0.011
	ASTM	0.004	0.006	0.003
	CRIM	0.008	0.012	0.009
	CRIMP	0.004	0.004	0.003
MSD	TOPP	0.014	0.016	0.017
	ASTM	0.012	0.014	0.014
	CRIM	0.013	0.016	0.016
	CRIMP	0.012	0.013	0.013

[a]SEE, standard error of the estimates; MAE, mean absolute error of the estimates for all bins; MSD, mean standard deviation of the estimates for all bins.
[b]TOPP, the Topp model; ASTM, American Society for Testing and Materials model; CRIM, the complex refractive index model; CRIMP, a piecewise CRIM model.

listed in Table 2. Besides, porosity observations were used in two approaches: (a) the estimated porosities after oven drying were directly used in the prediction of water content for each sample during the optimization; and (b) only a generalized porosity constant was used in the optimization, and it was set as the averaged value ($\bar{\Phi}_r$) of all the estimated porosities for each specific soil.

2.4 | Sensitivity analysis

Soil porosity is constructed differently in the three models—ASTM, CRIM, and CRIMP. To illustrate the role of porosity in model prediction, exemplifying sensitivity analysis was conducted with Monte Carlo simulations. Provided the same white noise $\sigma_\Phi = 0.03$ of the porosity $\Phi = 0.45$, there were 50 simulations conducted at each dielectric permittivity values for each model. The synthetic constants for each model are given as $a = 1.1$ and $b = 8.8$ for ASTM, $\varepsilon_s = 5$ and $\alpha = 0.5$ for CRIM, $\varepsilon_c = 20$, $\theta_{c,max} = 0.25$, and $\alpha = 0.5$ for CRIM.

To investigate the impact of the deviation of the generalized porosity constant on the calibration, a simple sensitivity analysis was conducted. Provided the same model fittings for each soil, the generalized porosity $\bar{\Phi}_r$ used in the optimization was replaced with four different values, $0.8\bar{\Phi}_r$, $0.9\bar{\Phi}_r$, $1.1\bar{\Phi}_r$, and $1.2\bar{\Phi}_r$ with a deviation of −20, −10, +10, and +20% in $\bar{\Phi}_r$, respectively.

2.5 | Error analysis

To assess the model predictive performance, three error metrics of model estimates are used in this study. As one of the most common metrics, the standard error of the estimates (SEE), is calculated as

$$\mathrm{SEE} = \sqrt{\frac{1}{N-2}\sum\left(\theta_n - \hat{\theta}_n\right)^2} \tag{4}$$

where N is the total number of employed measurements. To address the model differences in the error distribution over the saturation range, the entire range of measurements are divided into a series of K intervals—namely, "bins"—and the mean error of the M estimates and the standard deviation in the k bin are calculated as

$$\mathrm{ME_k} = \frac{1}{M}\sum\left(\theta_m - \hat{\theta}_m\right) \tag{5}$$

and

$$\sigma_k = \sqrt{\frac{1}{M-1}\sum\left(\theta_m - \hat{\theta}_m - \mathrm{ME_k}\right)^2} \tag{6}$$

Thus, the mean absolute error (MAE) and the mean standard deviation (MSD) over the entire range

$$\mathrm{MAE} = \frac{1}{K}\sum\left|\mathrm{ME_k}\right| \tag{7}$$

and

$$\mathrm{MSD} = \frac{1}{K}\sum\sigma_k \tag{8}$$

are derived for representing the error characteristics caused by bias and variance.

3 | RESULTS

3.1 | Soil porosity variation during calibrations

Figure 1 shows the variation of the porosity with the degree of water saturation for the eight soils during the calibration experiment. The blue and red curves were obtained from two trials with the same soil samples, and the discrepancy originated from different compaction pressures by two operators. Generally, the range of porosity variation for each soil varies from 0.06 to 0.14, and the evolution of the soil pore structure experiences two stages. At the first stage, the size and amount of soil aggregates both increase with the water content and result in a rapid increase of porosity untill the maximum one is reached. The corresponding water saturation and content

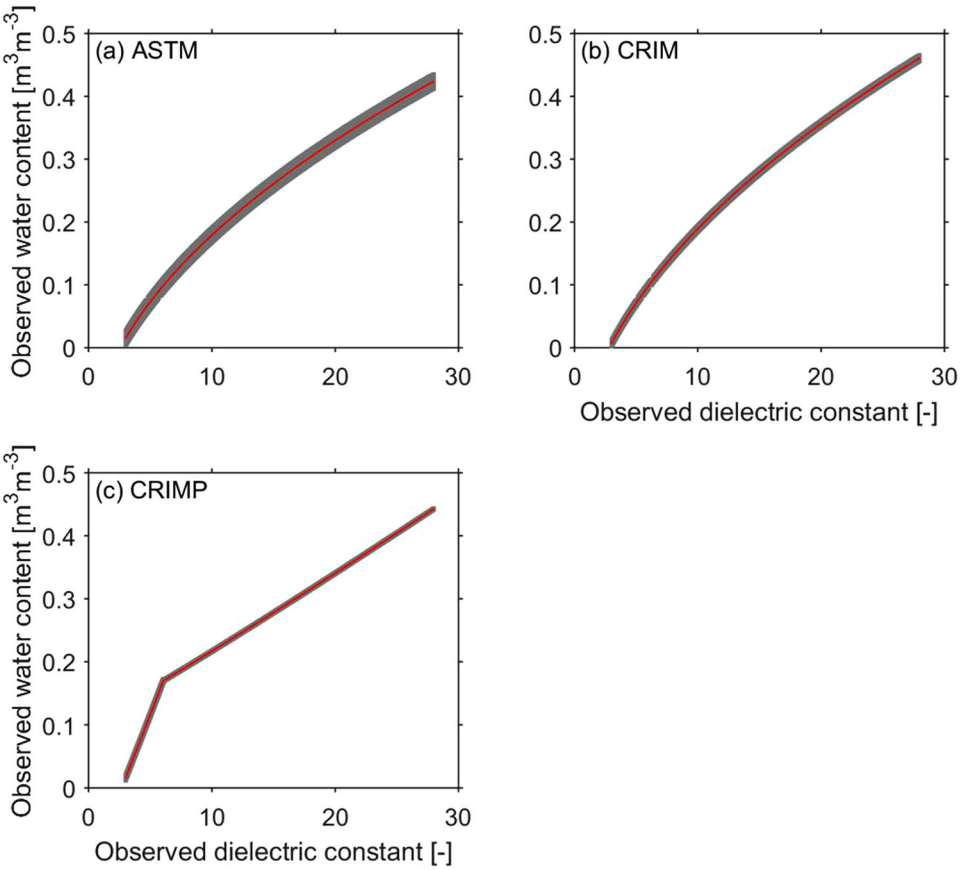

FIGURE 4 Theoretical illustration of the varying sensitivity of the porosity-dependent model prediction (the American Society for Testing and Materials model [ASTM], the complex refractive index model [CRIM], and a piecewise CRIM model [CRIMP]) to the porosity with white noise ($\sigma_\Phi = 0.03$) over the water dynamic range. Red curve: the model truth; gray curve: error bar of the Monte Carlo simulations

at the maximum porosity roughly increases from sandy soils to clayey soils. This is mainly attributed to the higher soil-specific surface area of clayey soils, which need more water to wet the grain surface than sandy soils. Then, at the second stage, more and more water lubricates the interface between soil particles and leads to a closer contact state. The porosity decreases gradually to a minimum (namely, the maximum compaction) around the liquid limit. Further increase in water content could easily lead to soil oversaturation and porosity increase, but such calibration is beyond the scope of this study.

3.2 | Residual structures of the calibrations using variable porosity

Figure 2 shows the fitting curves of the four models for the eight soils. We note that, since the porosity is used as a known variable in regression, these curves are different from that when porosity is assumed to be constant. Figure 3 shows the water content residuals between the observations and estimates ($\theta_r - \hat{\theta}_r$) for the three groups of soils (Part 1, Part 2, and all in Table 1). For better visualization of the residual structures, an error bar curve (red color) using MAE and MSD is added in each plot.

Results in Table 3 show that all the four models perform reasonably with a SEE of around 0.02 $m^3\ m^{-3}$ of the estimates. Generally, the performances of ASTM and CRIMP are better than those of TOPP and CRIM. Given a comparable white noise of about 0.015 $m^3\ m^{-3}$ in MSD, the differences among the models mainly originate from the structural biases, MAE, as shown in Figure 3. For the Part 1 soils, the residual structures of TOPP and CRIM show a similar pattern to the porosity variation in Figure 1, whereas it is more evident for the Part 2 soils with higher clay content.

As illustrated in Figure 4, the sensitivity analysis shows that the impact of porosity white noise varies differently among the models of ASTM, CRIM, and CRIMP. The predicted water content error ($\sigma_{\theta,ASTM} = 0.011\ m^3\ m^{-3}$) of ASTM is larger than the other two models ($\sigma_{\theta,CRIM} = 0.004\ m^3\ m^{-3}$, $\sigma_{\theta,CRIMP} = 0.001\ m^3\ m^{-3}$). Overall, the errors of ASTM and CRIM over the water dynamic range are uniform in statistics, and the CRIMP is also uniform in two segmented sections. However, CRIMP is not as sensitive as ASTM and CRIM to porosity change.

To our knowledge, the residual structures could be associated with the effects of bound water content and the systematic porosity variation. In comparison with TOPP, ASTM takes

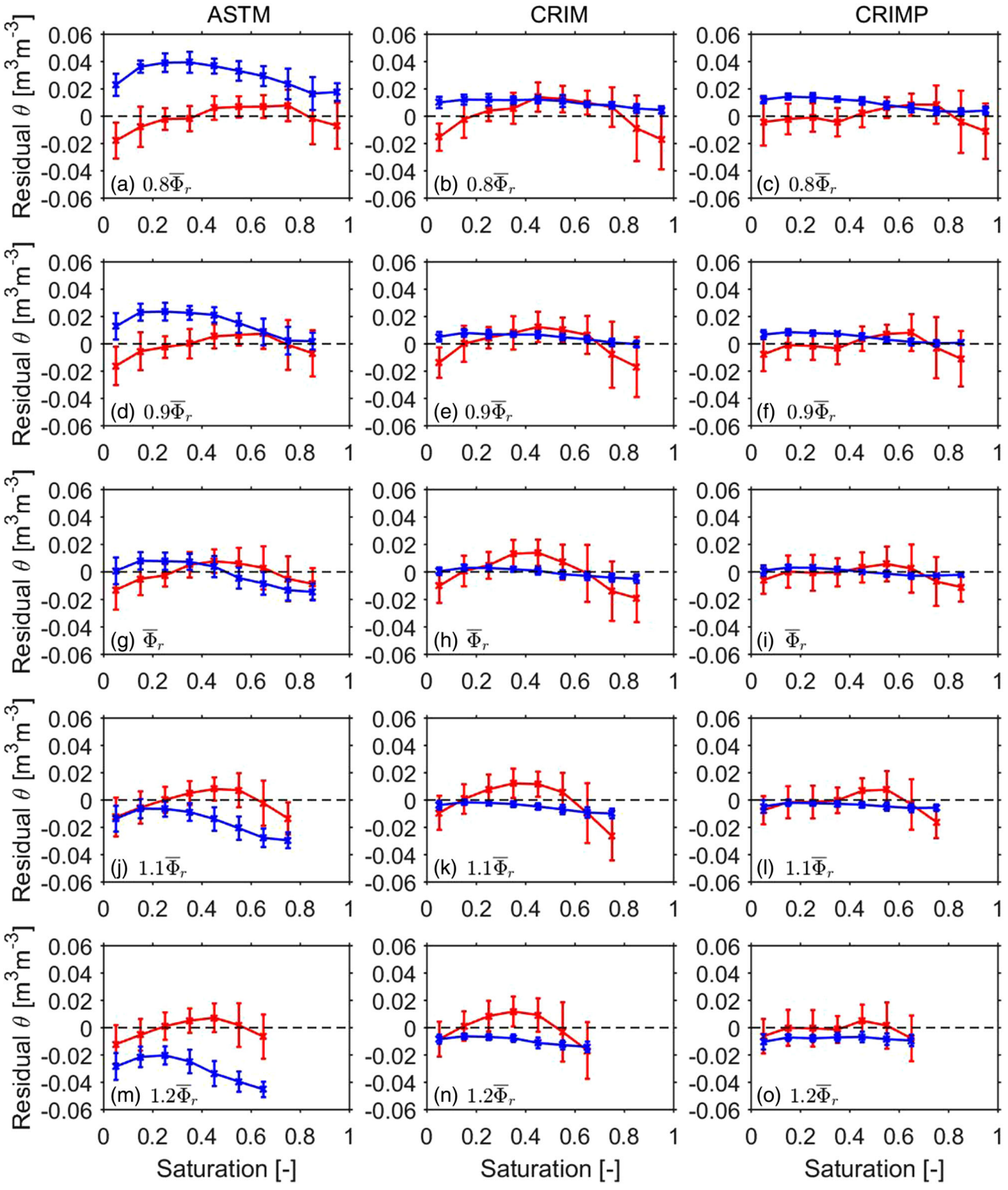

FIGURE 5 Evolution of the residual structures (red curve) of model estimates (the American Society for Testing and Materials model [ASTM], the complex refractive index model [CRIM], and a piecewise CRIM model [CRIMP]) when using a generalized porosity constant ranging from $0.8\bar{\Phi}_r$ to $1.2\bar{\Phi}_r$ for the Part 1 soils. The blue curves are the projected errors when replacing the corresponding generalized porosity constant with the observed variable porosity. θ stands for volumetric water content

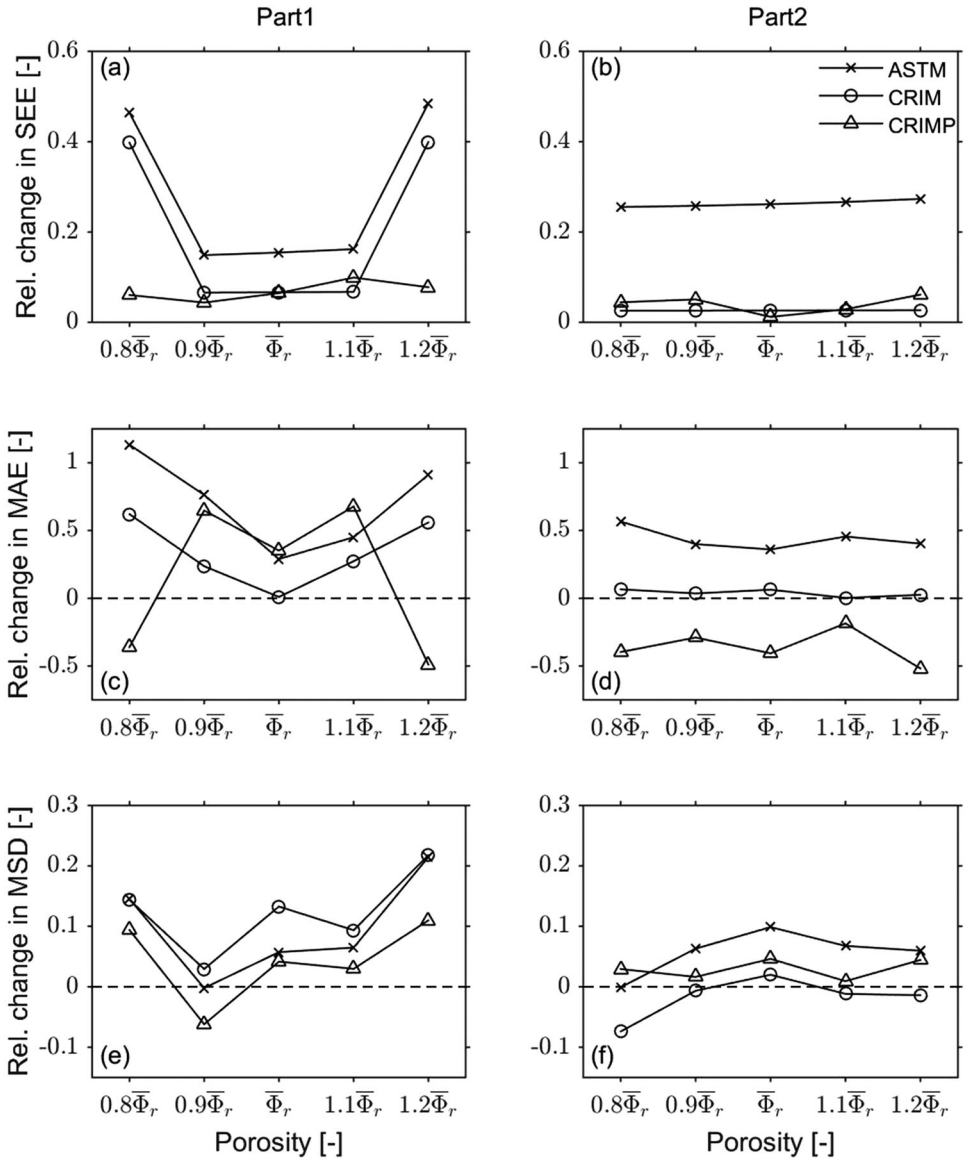

FIGURE 6 Contrast sensitivities of the three (the American Society for Testing and Materials model [ASTM], the complex refractive index model [CRIM], and a piecewise CRIM model [CRIMP]) model estimates to the deviation of the generalized porosity constant ($\bar{\Phi}_r$) for Part 1 and Part 2 soils. The relative changes of error metrics standard error of the estimate (SEE), mean absolute error (MAE), and mean standard deviation (MSD) are calculated in relative to the error metrics for the Part 1 and Part 2 soils in Table 3

into consideration of the porosity variation properly and effectively reduces the structural bias. Although CRIM has considered the porosity variation, the structural bias is still comparable with TOPP. This is mainly attributed to the weak role of porosity in the model structure of CRIM, whereas CRIMP further considers the bound water effect and yields the best result, though it has more parameters than ASTM.

3.3 | Residual structures of the calibrations using generalized porosity constant

In comparison with the above approach using variable porosity, the same model fittings of ASTM, CRIM, and CRIMP using generalized porosity constant were conducted for all the soils. Figure 5 demonstrates the performances of the three models using generalized porosities for Part 1 soils. The changes of residual pattern vary differently among the models of ASTM, CRIM, and CRIMP. The residual pattern of ASTM for the Part 1 soils in Figure 5g changes clearly in comparison with Figure 3d, where the changes mainly occur at the dry end. For better understanding, the projected errors purely induced by systematic porosity variation (blue curves) show an evident downward convex structure. There is no doubt that the porosity generalization does bring in additional structural biases and strengthen the residual patterns, whereas the residual patterns of CRIM in Figure 5h only slightly changes in

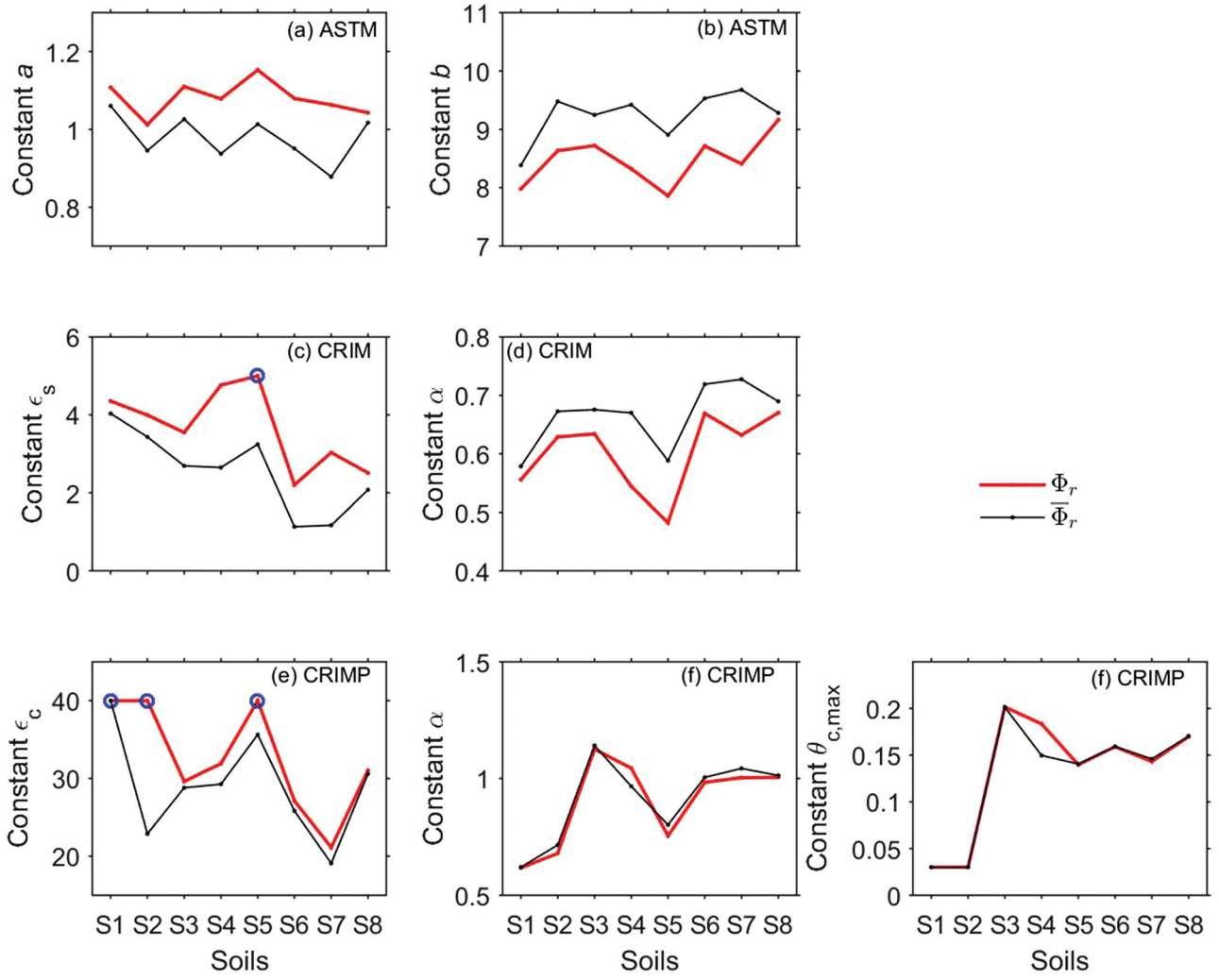

FIGURE 7 Comparison of the estimated calibration constants of the American Society for Testing and Materials model (ASTM), the complex refractive index model (CRIM), and a piecewise CRIM model (CRIMP) using variable porosity Φ_r and generalized porosity constant $\bar{\Phi}_r$

comparison with Figure 3g. In light of the segmented dielectric permittivity model of CRIMP, the generalized porosity constant deviation would also bring in additional structural bias. Its magnitude is not as significant as ASTM, but it would slightly modify the residual pattern. Thus, the porosity generalization only exerts a little impact on the residual patterns of CRIMP in Figure 5i.

The impact of the porosity generalization and its deviation on the model calibration is summarized in Figure 6 for both Part 1 and Part 2 soils. In general, a generalized porosity constant around $\bar{\Phi}_r$ yields the best calibration than the other deviated values. This is especially evident for the Part 1 soils. Besides, the standard errors, SEE, of all models increase when replacing the variable porosity with generalized porosity constant, but their magnitudes are different. The most significant one is ASTM, where the structural biases MAEs increased by 29 and 36% for the Part 1 and Part 2 soils, respectively. The relative change of MAEs for CRIM is negligible because the model is not so sensitive to porosity change.

In general, using the generalized porosity constant $\bar{\Phi}_r$ (arithmetic mean of the observed values) is preferred for all the models. Provided the role of porosity, ASTM is more susceptible to the porosity generalization than the other two models for practical application. In contrast, CRIMP does not show a strong sensitivity to the porosity generalization.

3.4 | Effect of porosity generalization on model built-in ability

Based on the statistical relations between calibration constants and some basic soil properties, some calibration models have the built-in ability that estimating these constants from readily available soil data like soil texture information (Drnevich et al., 2005; Ponizovsky et al., 1999), but the built-in ability relies not only on the model adequacy for the applied soils but also on some implicit preconditions like

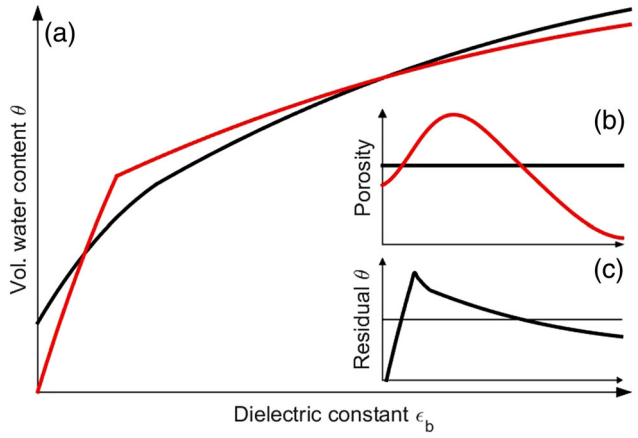

FIGURE 8 Conceptual illustration of the structural bias caused by porosity generalization in piecewise complex refractive index (CRIMP) model calibration. (a) Observed (red) and modeled (black) data curves for soil dielectric constant and water content; (b) the observed (red) and generalized (black) porosity over the saturation range; (c) residual curve between observed and modeled water content

porosity variation addressed in this study. Consequently, the two approaches accounting for porosity variation would bring in certain impacts on the calibration constants in comparison with the ideal case with invariable porosity.

Figure 7 compares the calibration constants estimated from the two approaches. Generally, the calibration constants of ASTM and CRIM deviate significantly for most of the investigated soils, although there is only a relatively small shift in the calibration constants of CRIMP. We note that some estimated constants (Figures 7c and 7e) marked with blue circles hit the upper boundary of the parameter setting range in the optimization. This is mainly attributed to the artifact of optimization due to limited data points. For instance, there are only two measurement points within the soil water content range dominated by bound water (Figures 1a and 1b). Overall, the comparison demonstrates that the built-in ability of CRIMP is relatively robust when using generalized porosity constant for soils with evident porosity variation.

4 | IMPLICATIONS FOR PRACTICAL APPLICATION

For practical application of the dielectric measurement techniques like TDR and GPR, the dielectric permittivity model selection is dependent on available information of field conditions and the user's requirement of measurement accuracy. For the laboratory calibration, porosity information is relatively easy to obtain, whereas the spatial and temporal information of soil porosity is usually not available for field application. Besides, it is also hard to keep a consistent porosity variation between laboratory calibration and field application. Hence, using a generalized porosity constant, as a rule of thumb, is preferred. However, the uncertainty in the generalized porosity constant might be problematic for the application of the dielectric permittivity models like ASTM with high sensitivity to porosity. Consequently, this limits their built-in abilities for the agricultural soils with systematic porosity variation.

Alternatively, provided models like CRIMP with a "perfect" structure for all soils, they are suggested to cope with the practical problems. Apart from the systematic porosity variation over the soil water dynamic range, another important feature of agricultural soils is the mediate to high clay and organic matter contents. The illustration of a typical relationship between dielectric constant and water content for such a soil is shown in Figure 8. The red line in Figure 8a is an idealized CRIMP model without random noises introduced into the calibration curve, and the black line stands for a CRIMP model fitting using a generalized porosity constant. A theoretical structural bias induced by the systematic porosity variation is shown in Figure 8c. From the above experiments for Part 1 and Part 2 soils, we know the structural bias index MAE is usually rather small. It allows an excellent accuracy of the measurements in the agricultural soils with systematic porosity variation, even using a roughly estimated value for the porosity constant in the model evaluation.

5 | CONCLUSIONS

This study investigated the commonly overlooked porosity variation with the degree of soil water saturation during the conventional laboratory calibration of TDR dielectric constant measurements. Through comparing with the calibration using detailed soil porosity information, we evaluated the viability of using a generalized porosity constant in the three preestablished dielectric permittivity models (ASTM, CRIM, and CRIMP) with different considerations of porosity. The findings are summarized as follows.

1. Soil porosity during the calibration experienced notable systematic variation from dry to nearly saturated and the pattern depends on the compaction operation and soil texture. The variation ranges from 0.06 to 0.14.
2. Using a generalized porosity constant would bring in additional structural bias in comparison with the calibration using variable porosity, and its magnitude depends on the model sensitivity to porosity (i.e., ASTM > CRIM > CRIMP). Deviation of the generalized porosity constant can further amplify the structural bias of ASTM and CRIM for the common soils with low clay content, but it is insensitive for the soils with high clay content due to the overwhelming role of model structure error.

3. Provided a relatively perfect model structure, the calibration selecting the models like CRIMP can work with a small standard error of around 0.01 m^3 m^{-3} and a negligible structural bias, and keep a stable built-in capability for estimating calibration constants from readily available soil data.

For practical application in agricultural lands, suitable model selection and calibration is essential to cope with the effect of porosity variation on the estimates of water content from dielectric technique measurements. However, we should keep in mind that the pattern of soil pore dynamics during the calibration was formed at the condition of discontinuously wetting of the remolded soil samples in the laboratory. It may vary differently under natural conditions induced by routine soil processes such as tillage, wetting–drying cycles, freezing–thawing cycles, and biological and chemical activities (Nimmo, 2004). The validity of the above findings needs to be further tested for field conditions.

ACKNOWLEDGMENTS

This work is financially supported by the NSFC (National Natural Science Foundation of China) Projects (Grants no. 41771262, 41671228).

AUTHOR CONTRIBUTIONS

Xicai Pan: Conceptualization; Formal analysis; Funding acquisition; Methodology; Project administration; Supervision; Writing-original draft; Writing-review & editing. Yudi Han: Data curation; Formal analysis; Investigation; Writing-review & editing. Kwok Pan Chun: Writing-review & editing. Jiabao Zhang: Supervision; Writing-review & editing. Donghao Ma: Resources; Writing-review & editing. Donghao Ma: Resources; Writing-review & editing. Hongkai Gao: Visualization; Writing-review & editing

CONFLICT OF INTEREST

The authors declare no conflict of interest.

ORCID

Xicai Pan https://orcid.org/0000-0003-3295-4629
Donghao Ma https://orcid.org/0000-0002-8573-2547

REFERENCES

Alakukku, L., Weisskopf, P., Chamen, W., Tijink, F., Van Der Linden, J., Pires, S., ... Spoor, G. (2003). Prevention strategies for field traffic-induced subsoil compaction: A review. Part 1. Machine/soil interactions. *Soil and Tillage Research*, *73*, 145–160. https://doi.org/10.1016/S0167-1987(03)00107-7

Alaoui, A., Lipiec, J., & Gerke, H. H. (2011). A review of the changes in the soil pore system due to soil deformation: A hydrodynamic perspective. *Soil and Tillage Research*, *115/116*, 1–15. https://doi.org/10.1016/j.still.2011.06.002

Blanco-Canqui, H., Lal, R., Post, W. M., Izaurralde, R. C., & Shipitalo, M. J. (2006). Organic carbon influences on soil particle density and rheological properties. *Soil Science Society of America Journal*, *70*, 1407–1414. https://doi.org/10.2136/sssaj2005.0355

Birchak, J. R., Gardner, C. G., Hipp, J. E., & Victor, J. M. (1974). High dielectric constant microwave probes for sensing soil moisture. *Proceedings of the Institute of Electrical and Electronics Engineers*, *62*, 93–98. https://doi.org/10.1109/PROC.1974.9388

Bremner, J. M., & Jenkinson, D. S. (1960). Determination of organic carbon in soil. I. Oxidation by dichromate of organic matter in soil and plant materials. *Journal of Soil Science*, *11*, 394–402. https://doi.org/10.1111/j.1365-2389.1960.tb01093.x

Chen, Y., & Or, D. (2006). Geometrical factors and interfacial processes affecting complex dielectric permittivity of partially saturated porous media. *Water Resources Research*, *42*(6). https://doi.org/10.1029/2005WR004744

Das, B. M. (2008). *Introduction to geotechnical engineering*. Toronto, ON, Canada: Thomson.

Datta, S., Taghvaeian, S., Ochsner, T. E., Moriasi, D., Gowda, P., & Steiner, J. L. (2018). Performance assessment of five different soil moisture sensors under irrigated field conditions in Oklahoma. *Sensors*, *18*(11). https://doi.org/10.3390/s18113786

Dobson, M. C., Ulaby, F. T., Hallikainen, M. T., & El-Rayes, M. A. (1985). Microwave dielectric behavior of wet soil: Part II. Dielectric mixing models. *IEEE Geoscience and Remote Sensing Society*, *GE-3*, 35–46. https://doi.org/10.1109/TGRS.1985.289498

Drnevich, V. P., Ashmawy, A. K., Yu, X., & Sallam, A. M. (2005). Time domain reflectometry for water content and density of soils: Study of soil-dependent calibration constants. *Canadian Geotechnical Journal*, *42*, 1053–1065. https://doi.org/10.1139/T05-047

Evett, S. R. (2000). The TACQ computer program for automatic time domain reflectometry measurements: II. Waveform interpretation methods. *Transactions of the ASAE*, *43*, 1947–1956. https://doi.org/10.13031/2013.3100

Fabiola, N., Giarola, B., da Silva, A., Imhoff, S., & Dexter, A. (2003). Contribution of natural soil compaction on hardsetting behavior. *Geoderma*, *113*, 95–108. https://doi.org/10.1016/S0016-7061(02)00333-6

Fleureau, J. M., Kheirbek-Saoud, S., Soemitro, R., & Taibi, S. (1993). Behavior of clayey soils on drying-wetting paths. *Canadian Geotechnical Journal*, *30*, 287–296. https://doi.org/10.1139/t93-024

Friedman, S. P. (1998). A saturation degree-dependent composite spheres model for describing the effective dielectric constant of unsaturated porous media. *Water Resources Research*, *34*, 2949–2961. https://doi.org/10.1029/98WR01923

Heimovaara, T. J. (1993). Design of triple-wire time domain reflectometry probes in practice and theory. *Soil Science Society of America Journal*, *57*, 1410–1417. https://doi.org/10.2136/sssaj1993.03615995005700060003x

Huisman, J. A., Hubbard, S. S., Redman, J. D., & Annan, A. P. (2003). Measuring soil water content with ground penetrating radar: A review. *Vadose Zone Journal*, *2*, 476–491. https://doi.org/10.2136/vzj2003.4760

Institute of Soil Science(ISS). (2001). *Chinese soil taxonomy*. Beijing: Science Press.

Jacobsen, O. H., & Schjønning, P. (1993). A laboratory calibration of time domain reflectometry for soil water measurements including effects of bulk density and texture. *Journal of Hydrology*, *151*, 147–157. https://doi.org/10.1016/0022-1694(93)90233-Y

Kaatze, U. 1989. Complex permittivity of water as a function of frequency and temperature. *Journal of Chemical and Engineering Data*, *34*, 371–374. https://doi.org/10.1021/je00058a001

Malicki, M. A., Plgge, R., & Roth, C. H. (1996). Improving the calibration of dielectric TDR soil moisture determination taking into account the solid soil. *European Journal of Soil Science*, *47*, 357–366. https://doi.org/10.1111/j.1365-2389.1996.tb01409.x

McNairn, H., Pultz, T. J., & Boisvert, J. B. (2002). Active microwave remote sensing methods. In J. H. Dane & G. C. Topp (Eds.), *Methods of soil analysis, Part 4: Physical methods* (pp. 475–488). Madison, WI: SSSA.

Nimmo, J. R. (2004). Porosity and pore size distribution. In D. Hillel (Ed.), *Encyclopedia of soils in the environment* (Vol. 3, pp. 295–303). London: Elsevier.

Or, D., Jones, S. B., Van Shaar, J. R., Humphries, S., & Koberstein, L. (2004). *User's guide WinTDR. Version 6.1*. Logan: Utah State University.

Ponizovsky, A. A., Chudinovaa, S. M., & Pachepsky, Y. A. (1999). Performance of TDR calibration models as affected by soil texture. *Journal of Hydrology*, *218*, 35–43. https://doi.org/10.1016/S0022-1694(99)00017-7

Radford, B., Bridge, B., Davis, R., McGarry, D., Pillai, U., Rickman, J.,… Yule, D. (2000). Changes in the properties of a Vertisol and responses of wheat after compaction with harvester traffic. *Soil and Tillage Research*, *54*, 155–170. https://doi.org/10.1016/S0167-1987(00)00091-X

Robinson, D. A., Campbell, C. S., Hopmans, J. W., Hornbuckle, B. K., Jones, S. B., Knight, R., … Wendroth, O. (2008). Soil moisture measurement for ecological and hydrological watershed-scale observatories: A review. *Vadose Zone Journal*, *7*, 358–389. https://doi.org/10.2136/vzj2007.0143

Robinson, D. A., Jones, S. B., Wraith, J. M., Or, D., & Friedman, S. P. (2003). A review of advances in dielectric and electrical conductivity measurement in soils using time domain reflectometry. *Vadose Zone Journal*, *2*, 444–475. https://doi.org/10.2136/vzj2003.4440

Roth, C. H., Malicki, M. A., & Plagge, R. (1992). Empirical evaluation of the relationship between soil dielectric constant and volumetric water content as the basis for calibrating soil moisture measurements by TDR. *Journal of Soil Science*, *43*, 1–13. https://doi.org/10.1111/j.1365-2389.1992.tb00115.x

Roth, K., Schulin, R., Fluhler, H., & Attinger, W. (1990). Calibration of time domain reflectometry for water content measurement using a composite dielectric approach. *Water Resources Research*, *26*, 2267–2273. https://doi.org/10.1029/WR026i010p02267

Schwing, M., Scheuermann, A., & Wagner, N. (2010). Experimental investigation of soil dielectric parameters during shrinkage. In K. Kupfer, et al. (Eds.), *Proceedings of the First European Conference on Moisture Measurement* (pp. 511–519). Weimar, Germany: MFPA Weimar.

Steelman, C. M., & Endres, A. L. (2011). Comparison of petrophysical relationships for soil moisture estimation using GPR ground waves. *Vadose Zone Journal*, *10*, 270–285. https://doi.org/10.2136/vzj2010.0040

Thomas, A. M., Chapman, D. N., Rogers, C. D. F., & Metje, N. (2010a). Electromagnetic properties of the ground: Part I—Fine-grained soils at the Liquid Limit. *Tunnelling and Underground Space Technology*, *25*, 714–722. https://doi.org/10.1016/j.tust.2009.12.002

Thomas, A. M., Chapman, D. N., Rogers, C. D. F., & Metje, N. (2010b). Electromagnetic properties of the ground: Part II—The properties of two selected fine-grained soils. *Tunnelling and Underground Space Technology*, *25*, 723–730. https://doi.org/10.1016/j.tust.2009.12.003

Topp, G. C., Davis, J. L., & Annan, A. P. (1980). Electromagnetic determination of soil water content and electrical conductivity measurement using time domain reflectometry. *Water Resources Research*, *16*, 574–582. https://doi.org/10.1029/WR016i003p00574

Weitz, A. M., Grauel, W. T., Keller, M., & E., Veldkamp (1997). Calibration of time domain reflectometry technique using undisturbed soil samples from humid tropical soils of volcanic origin. *Water Resources Research*, *33*, 1241–1249. https://doi.org/10.1029/96WR03956

How to cite this article: Pan X, Han Y, Chun KP, Zhang J, Ma D, Gao H. On the laboratory calibration of dielectric permittivity models for agricultural soils: Effect of systematic porosity variation. *Vadose Zone J.* 2021;20:e20096. https://doi.org/10.1002/vzj2.20096